Femtosecond-laser pumped CdSiP₂ optical parametric oscillator producing 100 MHz pulses centered at 6.2 m

Zhang, Zhaowei; Reid, Derryck Telford; Kumar, S. Chaitanya; Ebrahim-Zadeh, Majid; Schunemann, Peter G; Zawilski, Kevin T; Howle, Christopher R

Published in:
Optics Letters

DOI:
10.1364/OL.38.005110

Publication date:
2013

Femtosecond-laser pumped $CdSiP_2$ optical parametric oscillator producing 100 MHz pulses centered at 6.2 μm

Zhaowei Zhang,[1,*] Derryck T. Reid,[1] S. Chaitanya Kumar,[2] Majid Ebrahim-Zadeh,[2,3] Peter G. Schunemann,[4] Kevin T. Zawilski,[4] and Christopher R. Howle[5]

[1]*Scottish Universities Physics Alliance (SUPA), Institute of Photonics and Quantum Sciences, School of Engineering and Physical Sciences, Heriot-Watt University, Edinburgh EH14 4AS, UK*

[2]*ICFO—Institut de Ciencies Fotoniques, Mediterranean Technology Park, 08860 Castelldefels, Barcelona, Spain*

[3]*Institucio Catalana de Recerca i Estudis Avancats (ICREA), Passeig Lluis Companys 23, Barcelona 08010, Spain*

[4]*BAE Systems, MER15-1813, P.O. Box 868, Nashua, New Hampshire 03061, USA*

[5]*Defence Science and Technology Laboratory, Porton Down, Salisbury SP4 0JQ, UK*

**Corresponding author: z.zhang@hw.ac.uk*

Received September 2, 2013; revised November 2, 2013; accepted November 2, 2013; posted November 4, 2013 (Doc. ID 196851); published November 25, 2013

We report the first, to the best of our knowledge, femtosecond-laser-pumped optical parametric oscillator (OPO) based on the newly developed nonlinear crystal, $CdSiP_2$. The OPO was synchronously pumped by a mode-locked Yb:KYW/Yb:fiber master-oscillator power amplifier, providing 1.053 μm pump pulses with durations of 130 fs at a repetition rate of 100 MHz. The 0.5-mm-thick $CdSiP_2$ crystal was cut for a type-I noncritical interaction, providing a broad phase-matching bandwidth and ensuring excellent temporal overlap among the pump, signal, and idler pulses. The OPO generated signal pulses with a spectral coverage over 1260–1310 nm and mid-infrared idler pulses with a broad spectral coverage at 5.8–6.6 μm (6.2 THz). With a 2% output coupler (OC), the threshold pump power was 600 mW. At the maximum pump power of 1.6 W, 0.55 W was absorbed due to two-photon absorption and residual linear absorption in the $CdSiP_2$ crystal, 0.75 W was transmitted, and 53 mW signal power was extracted through the OC. We estimate that the generated idler power was 24 mW.

OCIS codes: (140.7090) Ultrafast lasers; (190.4410) Nonlinear optics, parametric processes; (190.4970) Parametric oscillators and amplifiers; (190.7110) Ultrafast nonlinear optics.

http://dx.doi.org/10.1364/OL.38.005110

Yb-based femtosecond-laser sources have shown themselves to be promising, power-scalable platforms for pumping optical parametric oscillators (OPOs) generating wavelengths in the mid-infrared (mid-IR) [1,2]. The extension of wavelength coverage to beyond 5 μm is made difficult by the lack of nonlinear materials combining transparency at the pump and idler wavelengths with suitable phase-matching and mechanical properties. Common oxide-based nonlinear crystals (e.g., $KTiOPO_4$ and $LiNbO_3$) perform well only below 4 μm, with the output power falling off significantly at longer wavelengths due to strong multiphonon absorption. To access the important long-wavelength mid-IR region at more than 4 μm, nonoxide crystals, such as $AgGaSe_2$, CdSe, $ZnGeP_2$, or orientation-patterned (OP) GaAs, need to be employed. Both $AgGaSe_2$ and CdSe are transparent from 0.75 to 15 μm, but to avoid two-photon absorption (TPA) during ultrashort pulse operation, they need to be pumped at above 1.5 μm by another OPO [3,4] or an Er^{3+} laser, and so are unable to take full advantage of Yb-based pump sources. Similarly, $ZnGeP_2$ and OP GaAs-based ultrafast OPOs need to be pumped with Tm^{3+} or Ho^{3+} lasers operating above 2.1 μm [5] or tandem-pumped by another OPO [6].

In this Letter, we introduce the first example of a femtosecond-laser-pumped OPO based on the newly developed nonlinear crystal, $CdSiP_2$ (CSP), which was recently identified as a promising material allowing efficient type-I phase-matched nonlinear conversion to >6 μm when pumped at near 1 μm [7–14]. Recent work on the phase-matching properties of CSP has even identified type-II and type-III routes to 9.5 μm using 1.064 μm pumping, validated by experimental difference frequency generation (DFG) data at wavelengths up to 9.5 μm [9]. These results, all of which were obtained in low-repetition-rate or *Q*-switched mode-locked regimes, motivated us to investigate the performance of CSP in a cw-mode-locked configuration, promising the possibility of continuous ultrabroadband mid-IR light for Fourier-transform and frequency-comb OPO spectroscopy.

CSP is transparent from 0.5 to 9 μm, and can be manufactured with high optical quality and low residual loss. It has a good thermal conductivity (13.6 $W\,K^{-1}\,m^{-1}$), facilitating high-power operation. The nonlinear coefficient of CSP ($d_{36} = 84.5\ pm\,V^{-1}$) is the highest among all nonlinear crystals that can be pumped at 1 μm [8]. Indeed, the nonlinear figure of merit (defined as d^2/n^3, where d is the nonlinear coefficient and n is the index of refraction) of CSP is ~300 $pm^2\,V^{-2}$ [8], among the best of all known nonlinear optical crystals. For comparison, the nonlinear figure of merit of PPLN is ~60 $pm^2\,V^{-2}$. In addition, CSP is the only nonlinear crystal that can offer noncritical phase matching (NCPM) for a 1 μm-pumped OPO with an idler output in the 6 μm region.

The synchronously pumped CSP OPO was based on the configuration shown in Fig. 1. The pump source (described further in [15]) comprised a 100 MHz semiconductor saturable absorber mirror (SESAM) mode-locked Yb:KYW master laser, followed by a Yb-doped fiber amplifier, and a pair of transmission gratings for pulse compression. The –3 dB pulse duration was measured to be 130 fs, and the spectrum had a central wavelength

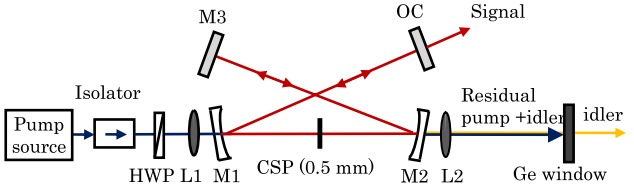

Fig. 1. OPO layout. HWP, half-wave plate; M, mirror; L, lens; OC, output coupler.

at 1053 nm and a −10 dB bandwidth of 27 nm (7.3 THz). After passing through a Faraday rotator, the maximum average pump power was 1.7 W. The pump was linearly polarized, and the polarization direction could be controlled by a half-wave plate.

The CSP crystal was cut at $\theta = 90°$, $\varphi = 45°$ for type-I ($e \rightarrow o + o$) NCPM and had a thickness of 0.5 mm. Its aperture was 4 mm × 5 mm. Both crystal surfaces were antireflection (AR) coated with a single-layer sapphire coating (TwinStar Optics), providing high transmission (>99%) for the pump and signal from 1035 to 1300 nm and high transmission (>95%) for the idler over 5900–6700 nm. In the four-mirror OPO cavity (Fig. 1), the focusing mirrors M1 and M2 (radius of curvature of 100 mm) and plane mirror M3 were coated on CaF_2 substrates for high transmission at the pump ($T > 95\%$ at 1020–1070 nm) and high reflectivity at the signal wavelength ($R > 99.8\%$ at 1.16–1.6 μm). The mirror coating was made of an oxide material, which presented a significant absorption at the idler wavelengths (estimated to be >40% at 5900–6700 nm). The pump beam was tightly focused by a convex lens L1 with a focal length of 50 mm, and had a Gaussian diameter of 60 μm in the position of the CSP crystal. The OPO was singly resonant for the signal, which was extracted via a 2% output coupler (OC). Since both surfaces of the CSP crystal had a (measured) signal reflection loss of 0.6%, the power extracted from the OC, with a transmission of 2%, accounted for only 45% of the generated signal. The cavity length was adjusted for synchronism with the 100 MHz repetition rate of the pump laser. The idler and residual pump passed through M2 and were collimated by an uncoated CaF_2 lens L2, followed by an AR-coated Ge window used to block all the residual pump prior to the idler diagnostics.

The high nonlinear coefficient of the CSP crystal and the extremely high pump intensity enabled by using femtosecond pump pulses and tight focusing ensure that an OPO with a thin nonlinear crystal can oscillate at a moderate average pump power. One benefit of using a thin nonlinear crystal is the broad phase-matching bandwidth. For a CSP crystal with a thickness of 0.5 mm and at a pump wavelength of 1055 nm, the −3 dB phase-matching bandwidths for the signal and idler are 28 and 663 nm, respectively. Figure 2 shows phase-matching efficiency plots for pump wavelengths from 1040 to 1070 nm, which allow signal (idler) tuning from 1285 to 1295 nm (6150–6400 nm).

The other benefit of using such a thin nonlinear crystal is that the temporal walk-off between the interacting pulses and their intrapulse group-delay dispersion are reduced, ensuring good temporal pulse overlap and limited pulse broadening. Based on the Sellmeier equations reported in [9], the pump–signal and pump–idler

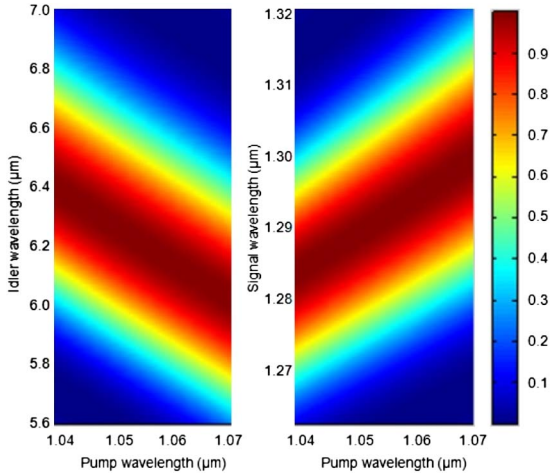

Fig. 2. Noncritical ($\theta = 90°$) type-I ($e \rightarrow o + o$) phase-matching efficiency maps for a 0.5-mm-thick CSP crystal at pump wavelengths from 1040 to 1070 nm.

temporal walk-off through the 0.5-mm-thick CSP crystal are +10 and −70 fs, respectively, much shorter than the pump pulse duration of 130 fs, implying excellent temporal overlap among the three interacting waves. The absolute group-delay dispersions at the pump, signal, and idler wavelengths are 743 fs^2, 532 fs^2, and −250 fs^2 respectively, imposing only a relatively small shaping effect on these pulses.

The band edge of CSP is close to 500 nm, implying that pumping near 1000 nm, with broadband high-intensity pulses, may cause TPA. Measuring the transmission of the *e*-polarized pump beam through the CSP crystal, we observed that the transmission dropped significantly with increasing pump intensity, verifying the presence of TPA. The supporting data, reproduced in Fig. 3, implied a TPA coefficient of 8.3 $cm\,GW^{-1}$ for the pump pulses, which had durations of 130 fs and a central wavelength of 1053 nm. In comparison, a TPA coefficient of 2.4 $cm\,GW^{-1}$ was reported for pump pulses at a similar central wavelength but with durations of 8.6 ps [13]. This TPA behavior limited the ability to scale the output of the CSP OPO by increasing the pump power; however, it did not destabilize the OPO operation, due to the good thermal conductivity of the crystal. In a separate

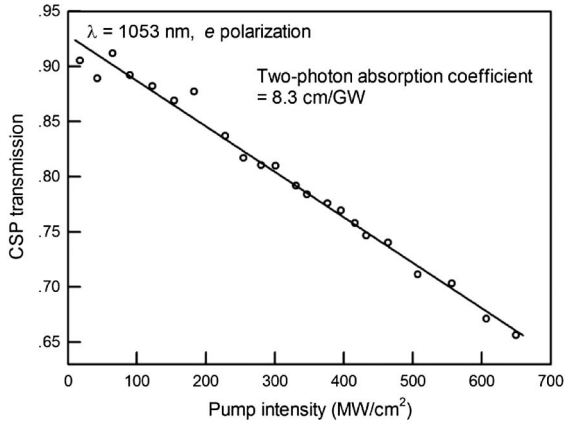

Fig. 3. Transmission through the 0.5-mm-thick CSP crystal as a function of intensity for the *e*-polarized 130 fs pump pulses.

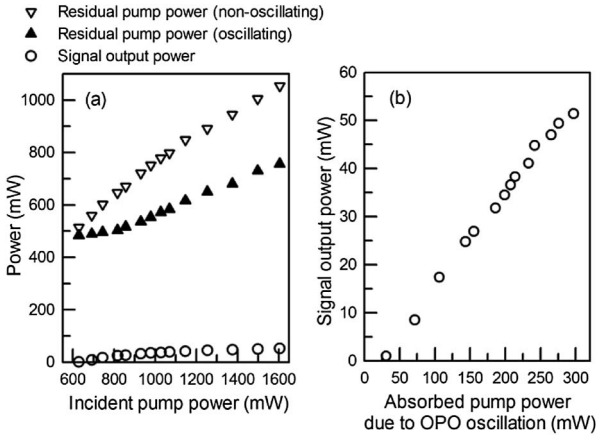

Fig. 4. (a) Measured signal output power from the OC, residual pump power when the OPO was oscillating, and residual pump power when the OPO was not oscillating versus incident pump power. (b) Measured signal output power from the OC versus the absorbed pump power due to OPO oscillation.

measurement, we confirmed that there was no TPA for similar intensities at the signal wavelength of 1.275 μm.

With the 2% OC, the threshold pump power was 600 mW. Figure 4(a) shows the signal output power measured after the OC, and the residual pump powers measured after lens L2 when the OPO was oscillating/blocked. At the maximum pump power of 1.6 W, 0.55 W (~34%) was absorbed due to TPA and residual linear loss in the CSP crystal, 0.75 W (47%) was transmitted, and only 0.30 W (19%) was converted in the nonlinear parametric interaction. Figure 4(b) shows the output-coupled signal power as a function of the pump power converted by parametric oscillation, indicating an extraction efficiency of ~20%. A maximum output-coupled signal power of 53 mW was measured; however, crystal reflection losses contribute a further 2.4% loss, and therefore we estimate that the total generated signal power was 118 mW.

The output signal spectrum from the OPO, pumped at full power, is shown in Fig. 5(a). Its central wavelength was 1275 nm, with a −10 dB bandwidth of 33 nm (6.1 THz), supporting transform-limited pulses with durations of approximately 170 fs. We believe the signal pulses were slightly chirped, since no dispersion compensation optics were employed, and the round-trip dispersion of the OPO cavity is estimated to be approximately +930 fs^2, contributed by the CSP crystal and the slight negative dispersion from the high-reflection mirrors. This broad signal bandwidth is due to the broad pump bandwidth [Fig. 5(b)] and the large phase-matching bandwidth of the CSP crystal. The incident pump (dashed line, measured in front of lens L1) and residual pump (solid line, measured after lens L2) spectra at full pump power are shown in Fig. 5(b) for comparison. It is clear that nonlinear frequency conversion occurs over the full pump spectrum range, confirming the large phase-matching bandwidth of the thin CSP crystal.

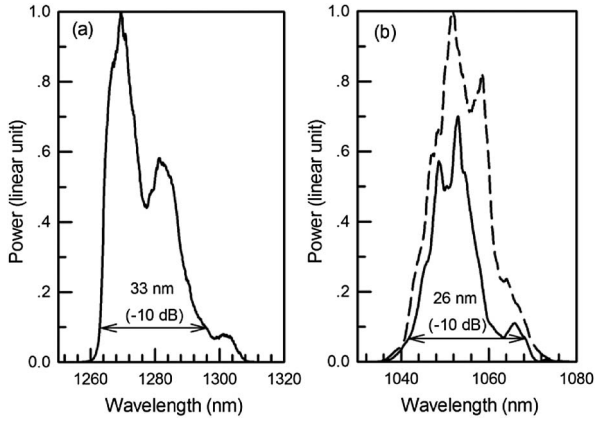

Fig. 5. (a) Signal spectrum at full pump power. (b) Spectrum of the incident pump (dashed line) and the residual pump (solid line).

Applying the Manley–Rowe relations (assuming signal and idler wavelengths of 1275 and 6200 nm, respectively), the generated idler power is expected to be ~24 mW. However, the idler power after the Ge window was too low to be measured by a thermal power meter with a sensitivity of 0.01 mW. For this reason we believe that nearly all the generated idler was absorbed by the multilayer oxide coating of the CaF_2 mirror. A mirror coated with a material (e.g., ZnSe) that is transparent to long-wave mid-IR is required to extract most of the generated idler power. Despite this, the 6.2 μm idler after the Ge window could be detected by a mercury cadmium telluride (MCT) photovoltaic detector operating within the 2–11 μm range. We measured the idler spectrum at full pump power by use of a Fourier-transform infrared (FTIR) spectrometer based on the MCT detector. A He–Ne laser with a central wavelength at 632.8 nm was coupled to the interferometer for absolute frequency calibration. As shown by the solid line of Fig. 6, the idler spectrum is rather broad, with a spectral coverage over 5.8–6.6 μm (6.2 THz), supporting transform-limited pulses with durations of approximately 160 fs. It is well known that there is strong absorption by atmospheric water vapor in this

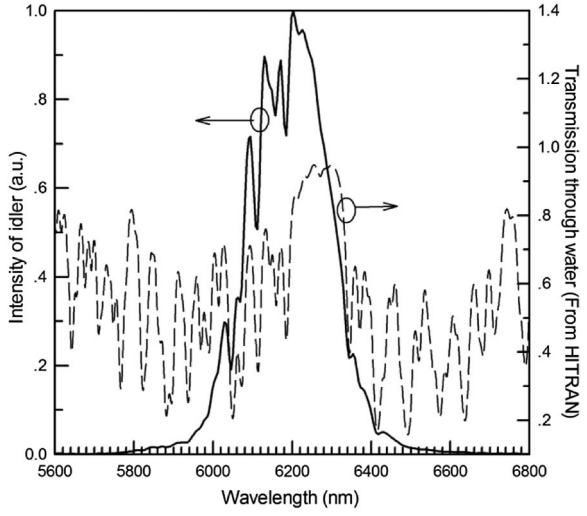

Fig. 6. Solid line: idler spectrum measured by an FTIR spectrometer. Dashed line: simulated transmission spectrum through water vapor, based on the HITRAN database, with a water concentration of 1% at one atmospheric pressure, a path length of 1.4 m, and a resolution (matching experiment) of 2.5 cm^{-1} (~10 nm).

spectral region. The generated idler traveled a path length of 1.4 m in air before being detected, and in Fig. 6, we also show the simulated transmission spectrum through water vapor, based on the HITRAN database, with a water concentration of 1% at one atmospheric pressure and a path length of 1.4 m. The characteristic absorption features of the water absorption are revealed in the measured idler spectrum. For both the acquisition of the idler spectrum and the simulation of water–vapor transmission, the spectral resolution was 2.5 cm^{-1} (~10 nm).

In summary, we have demonstrated, to the best of our knowledge, the first femtosecond-laser pumped $CdSiP_2$ OPO. Pumped by a Yb:KYW/Yb:fiber master-oscillator power amplifier delivering 130 fs pulses at 1.053 μm, it generated a broadband signal spectrum over 1260–1310 nm and a broadband idler spectrum from 5.8 to 6.6 μm. At full pump power, the total generated signal (idler) powers were estimated to be 118 mW (24 mW). We observed strong TPA in the CSP crystal for the femtosecond pump pulses near 1.05 μm, which, however, did not undermine the stability of OPO oscillation. To alleviate or avoid TPA, pump sources operating at longer wavelengths are required, e.g., by use of a Raman-shifted Yb: fiber system [16], a mode-locked Cr:Forsterite laser [17], or a mode-locked Er:fiber laser system [18]. Moreover, there is also potential for generating broadband mid-IR emission at the 6–9 μm region from a CSP OPO by use of a critical phase-matching scheme. The potential applications of broadband mid-IR coherent source generated from the CSP OPO include FTIR spectroscopy, mid-IR frequency-comb spectroscopy, and sensitive detection of gas- and liquid-phase chemical species [19–21].

The authors gratefully acknowledge financial support from the Centre for Defence Enterprise, part of the UK Ministry of Defence.

References

1. T. P. Lamour, L. Kornaszewski, J. H. Sun, and D. T. Reid, Opt. Express **17**, 14229 (2009).
2. F. Adler, K. C. Cossel, M. J. Thorpe, I. Hartl, M. E. Fermann, and J. Ye, Opt. Lett. **34**, 1330 (2009).
3. S. Marzenell, R. Beigang, and R. Wallenstein, Appl. Phys. B **69**, 423 (1999).
4. M. A. Watson, M. V. O'Connor, D. P. Shepherd, and D. C. Hanna, Opt. Lett. **28**, 1957 (2003).
5. N. Leindecker, A. Marandi, R. L. Byer, K. L. Vodopyanov, J. Jiang, I. Hartl, M. Fermann, and P. G. Schunemann, Opt. Express **20**, 7046 (2012).
6. J.-B. Dherbecourt, A. Godard, M. Raybaut, J.-M. Melkonian, and M. Lefebvre, Opt. Lett. **35**, 2197 (2010).
7. K. T. Zawilski, P. G. Schunemann, T. C. Pollak, D. E. Zelmon, N. C. Fernelius, and F. K. Hopkins, J. Cryst. Growth **312**, 1127 (2010).
8. V. Petrov, Opt. Mater. **34**, 536 (2012).
9. V. Kemlin, P. Brand, B. Boulanger, P. Segonds, P. G. Schunemann, K. T. Zawilski, B. Ménaert, and J. Debray, Opt. Lett. **36**, 1800 (2011).
10. V. Petrov, G. Marchev, P. G. Schunemann, A. Tyazhev, K. T. Zawilski, and T. M. Pollak, Opt. Lett. **35**, 1230 (2010).
11. A. Peremans, D. Lis, F. Cecchet, P. G. Schunemann, K. T. Zawilski, and V. Petrov, Opt. Lett. **34**, 3053 (2009).
12. O. Chalus, P. G. Schunemann, K. T. Zawilski, J. Biegert, and M. Ebrahim-Zadeh, Opt. Lett. **35**, 4142 (2010).
13. S. Chaitanya Kumar, A. Agnesi, P. Dallocchio, F. Pirzio, G. Reali, K. T. Zawilski, P. G. Schunemann, and M. Ebrahim-Zadeh, Opt. Lett. **36**, 3236 (2011).
14. S. Chaitanya Kumar, M. Jelínek, M. Baudisch, K. T. Zawilski, P. G. Schunemann, V. Kubeček, J. Biegert, and M. Ebrahim-Zadeh, Opt. Express **20**, 15703 (2012).
15. Z. Zhang, J. Sun, T. Gardiner, and D. T. Reid, Opt. Express **19**, 17127 (2011).
16. T. W. Neely, T. A. Johnson, and S. A. Diddams, Opt. Lett. **36**, 4020 (2011).
17. Y. Pang, B. I. Minkov, V. Yanovsky, and F. Wise, Opt. Lett. **18**, 1168 (1993).
18. K. Tamura, E. P. Ippen, H. A. Haus, and L. E. Nelson, Opt. Lett. **18**, 1080 (1993).
19. K. A. Tillman, R. R. J. Maier, D. T. Reid, and E. D. McNaghten, Appl. Phys. Lett. **85**, 3366 (2004).
20. F. Adler, P. Masłowski, A. Foltynowicz, K. C. Cossel, T. C. Briles, I. Hartl, and J. Ye, Opt. Express **18**, 21861 (2010).
21. Z. Zhang, T. Gardiner, and D. T. Reid, Opt. Lett. **38**, 3148 (2013).